STRIPLINE MAGNETIC MODULATORS FOR LASERS AND ACCELERATORS

W. C. Nunnally
Los Alamos National Laboratory
Los Alamos, NM 87545

Abstract

The basics of magnetic modulators including magnetic element and circuit considerations as applied to accelerators and lasers requiring repetitive (1-10 kHz), high voltage (50-500 kV), short pulse (50-100 ns) are discussed. The scaling of energy losses and switching parameters with material are included.

Introduction

The generation of very high peak power pulses in a reliable manner at high-repetition rates is essential to many high-energy research programs involving lasers and accelerators. Conventional technology is unable to provide the multigigawatt, multikilohertz power conditioning systems with the required reliability and lifetime, primarily because conventional switching components cannot operate simultaneously at the voltages, currents, and repetition rates required. Saturable ferromagnetic elements can be used to compress low-power pulses into multigigawatt pulses at multikilohertz repetition rates. Thus, a magnetic modulator consisting of several sequential, saturable, magnetic element stages can be used to shift conventional switch operating parameters from the multigigawatt output level to a much lower input power level at which existing repetitive switches can function.

Magnetic Modulator Basics

Saturable Ferromagnetic Element (SFME)

The simplest SFME or magnetic switch is the saturable inductor, shown in Fig. 1. When the switch is closed at time, t = 0, the impedance of the saturable inductor is large so that the load current and voltage are small, with most of the voltage appearing across the large unsaturated inductance.

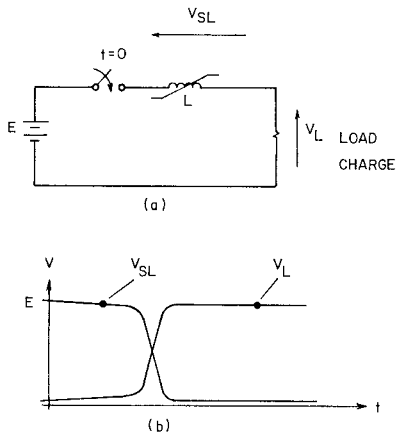

Fig. 1. Magnetic switch characteristics.

After the flux content of the magnetic material in the core is exceeded, the magnetic material saturates, reducing the series impedance of the SFME by several orders of magnitude, and a majority of the source voltage appears across the load. The circuit of Fig. 1 illustrates an important characteristic of SFME circuits; a conventional switch is required at some point in the system because the SFME can hold off dc voltage for only a finite period of time.

Basic Resonant Energy Transfer

A basic resonant energy transfer circuit used in magnetic modulator circuits is shown in Fig. 2.

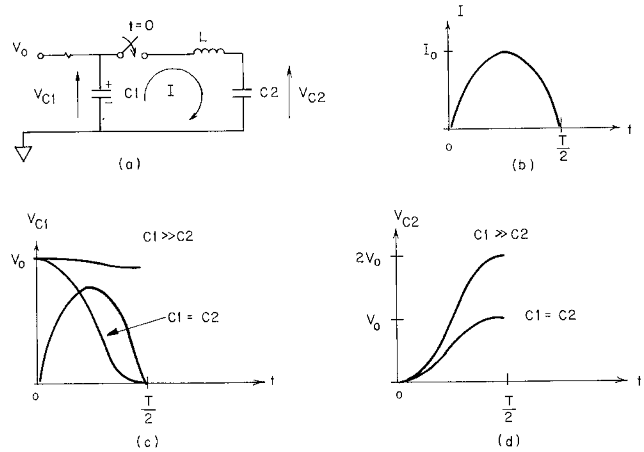

Fig. 2. Basic resonant energy transfer circuit.

If C1 = C2 without losses, all the energy stored in C1 at voltage V_o is transferred to C2 at time = T/2, which is then charged to voltage V_o. The important point to make is that the maximum energy transferred E_T at voltage V_o in a resonant time T/2 is given by[1]

$$E_T = \left(\frac{V_o T}{2\pi}\right)^2 \frac{1}{L_T} \tag{1}$$

where L_T is the total series inductance. Thus, the total inductance of the SFME and circuit must be designed sufficiently low to transfer a specific energy in time T/2 at voltage V_o.

Basic Magnetic Modulator Circuits

Series Magnetic Pulse Compressor

The three-stage series magnetic pulse compressor circuit[1] shown in Fig. 3 provides near-unity energy transfer when the stage capacitances are equal and time compression of the input pulse at constant voltage. The primary switch must operate at the output voltage but at reduced current and rate of current change. The repetition rate of the system is still limited by the conventional primary switch.

Parallel Magnetic Pulse Compressor

The parallel magnetic pulse compression circuit[1] shown in Fig. 4 uses saturable transformers to provide voltage gain so that the primary switch can operate at low voltage while the circuit produces the high voltages required by lasers and accelerators. Near-unity energy transfer is obtained by matching the successive capacitors through the transformer turns ratios. The output pulse is compressed in time at constant peak current so that the primary switch must conduct the peak load current but hold off much lower voltages.

Report Documentation Page	*Form Approved* *OMB No. 0704-0188*

1. REPORT DATE	2. REPORT TYPE	3. DATES COVERED
JUN 1981	**N/A**	**-**

4. TITLE AND SUBTITLE	
Stripline Magnetic Modulators For Lasers And Accelerators	5a. CONTRACT NUMBER
	5b. GRANT NUMBER
	5c. PROGRAM ELEMENT NUMBER
6. AUTHOR(S)	5d. PROJECT NUMBER
	5e. TASK NUMBER
	5f. WORK UNIT NUMBER
7. PERFORMING ORGANIZATION NAME(S) AND ADDRESS(ES) **Los Alamos National Laboratory Los Alamos, NM 87545**	8. PERFORMING ORGANIZATION REPORT NUMBER
9. SPONSORING/MONITORING AGENCY NAME(S) AND ADDRESS(ES)	10. SPONSOR/MONITOR'S ACRONYM(S)
	11. SPONSOR/MONITOR'S REPORT NUMBER(S)

12. DISTRIBUTION/AVAILABILITY STATEMENT
Approved for public release, distribution unlimited

13. SUPPLEMENTARY NOTES
See also ADM002371. 2013 IEEE Pulsed Power Conference, Digest of Technical Papers 1976-2013, and Abstracts of the 2013 IEEE International Conference on Plasma Science. Held in San Francisco, CA on 16-21 June 2013. U.S. Government or Federal Purpose Rights License.

14. ABSTRACT
The basics of magnetic modulators including magnetic element and circuit considerations as applied to accelerators and lasers requiring repetitive (1-10 kHz), high voltage (50-500 kV), short pulse (50-100 ns) are discussed. The scaling of energy losses and switching parameters with material are included.

15. SUBJECT TERMS

16. SECURITY CLASSIFICATION OF:			17. LIMITATION OF ABSTRACT	18. NUMBER OF PAGES	19a. NAME OF RESPONSIBLE PERSON
a. REPORT **unclassified**	b. ABSTRACT **unclassified**	c. THIS PAGE **unclassified**	**SAR**	**4**	

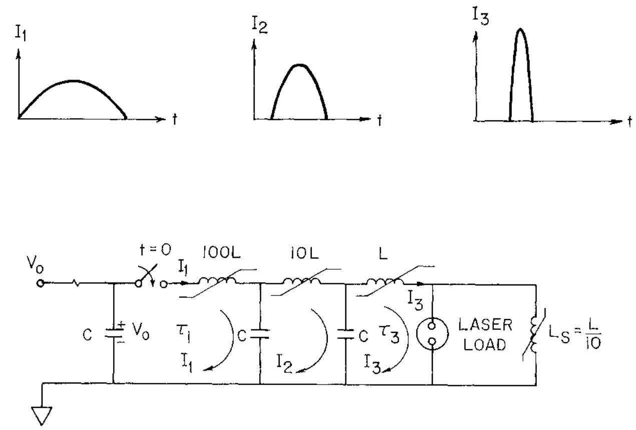

CURRENT GAIN $= \frac{I_3}{I_1} = (50)^{1/2} \simeq 7$

PULSE COMPRESSION $= \frac{\tau_1}{\tau_3} = (50)^{1/2} \simeq 7$

ENERGY TRANSFER EFFICIENCY $= \frac{\epsilon_3}{\epsilon_1} \simeq 1.0$

Fig. 3. Series magnetic pulse compressor circuit.

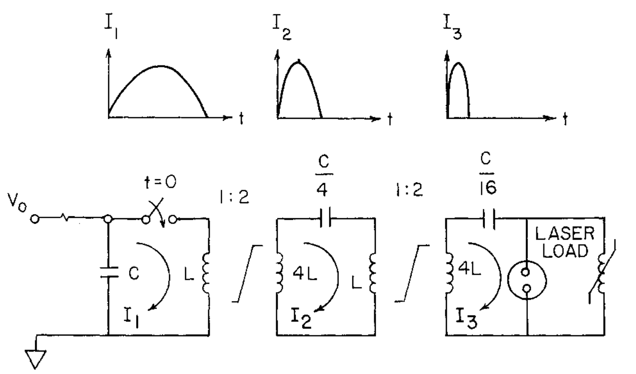

VOLTAGE GAIN = 4

PULSE COMPRESSION = 4

ENERGY TRANSFER EFFICIENCY $\simeq \frac{\epsilon_3}{\epsilon_1} \times 100 \simeq 100\%$

Fig. 4. Parallel magnetic pulse compressor circuit.

The parallel pulse compression circuit is logical choice for delivering repetitive, high-voltage pulses to lasers and accelerator loads because a low voltage solid state device can be used as the primary switch to increase system reliability and lifetime. The development of a low-inductance, saturable transformer that has a high primary to secondary coupling coefficient is the real limitation and challenge of the parallel magnetic pulse compressor circuit.

Transmission-Line Magnetic Pulse Compressor

A modification of the series pulse compressor circuit of Fig. 3 is the transmission-line magnetic pulse compressor shown in Fig. 5. This circuit is used to shape and compress a slow input pulse and deliver a rectangular pulse to the load.

General Circuit Observations

A combination of the above circuits can be used to deliver the required pulse to the load. The parallel circuit would be used for voltage gain and the low-voltage primary switch advantage. The series circuit is for sinusoidal pulse compression at constant voltage, and the transmission-line circuit for pulse shaping. Note that a standard pulse transformer or a dual

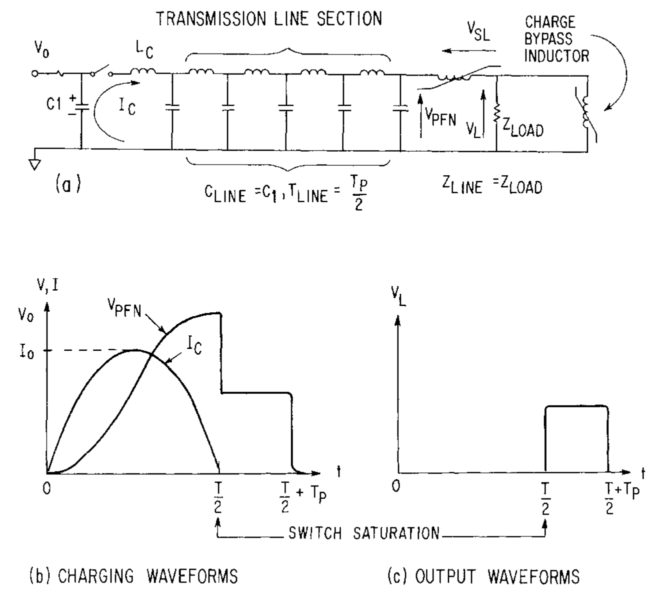

Fig. 5. Transmission-line magnetic pulse compressor circuit.

resonance (k = 0.6) transformer can be used to obtain voltage gain in the early stages if the required resonant period (sufficiently low inductance) can be obtained.

Low-Inductance Design

As discussed previously, the maximum total circuit inductance is determined by the energy to be transferred, E_T at peak voltage, V_0 in time T/2. The total inductance is composed of the capacitor inductances, the saturated inductance of one or more magnetic elements, and stray inductances, all of which must be minimized. The saturated inductance of a magnetic element can be defined by

$$L_{sat} = \frac{\mu_0 \mu_{sat} A_T N_T^2}{\ell_w} , \tag{2}$$

where A_T is the total cross-sectional area of the magnetic material and interlaminar insulation. The total cross-sectional area is approximately equal to the magnetic material cross section A_m determined from flux conservation. The magnetic material cross section is chosen to prevent saturation of the magnetic element during the previous stage operation or

$$A_m = \frac{1}{\Delta B \ N_T} \int_0^{T_{sat}} V(t)dt , \tag{3}$$

where ΔB is the magnetic material flux swing, and V(t) is the voltage applied to the magnetic element prior to saturation at time = T_{sat}. Because the value of μ_{sat} is between 1 and 3, the only variables available to obtain the desired value of L_{sat} are the number of conductor turns N_T and the width of the conductor turn ℓ_w. To minimize L_{sat}, the number of turns is limited to 1 or 2, and the winding width is increased to form the standard low-inductance stripline geometry. Stripline geometry also facilitates lower capacitor inductance through parallel units and reduced stray inductance. Two single-turn, low-inductance geometries are shown in Fig. 6.

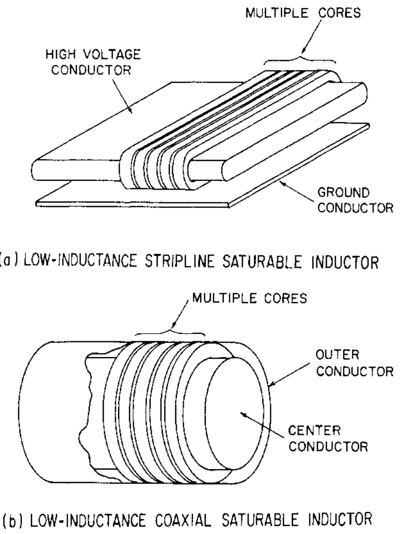

Fig. 6. Low-inductance SFME geometries.

Ferrites can be used for the magnetic core material. Note that because the available flux swing ΔB for ferrites is approximately one-third that for steel, the conductor width must also be increased by a factor of 3 to obtain the same inductance and thus transfer the same energy. The approximate ferrite volume is thus 10 times that required for a magnetic element using steel magnetic material. Therefore only steel magnetic materials are considered in this paper.

Magnetic Material Considerations

Switching Considerations

In the short-pulse, high-voltage applications being considered, the magnetic material is driven several hundred to several thousand times the saturation magnetic field in a time much less than the diffusion time. Under these conditions, the state of the magnetic material changes as a steep saturation front propagates into the thin-metal laminations. The spatial distribution of the relevant parameters during saturation is illustrated in Fig. 7.

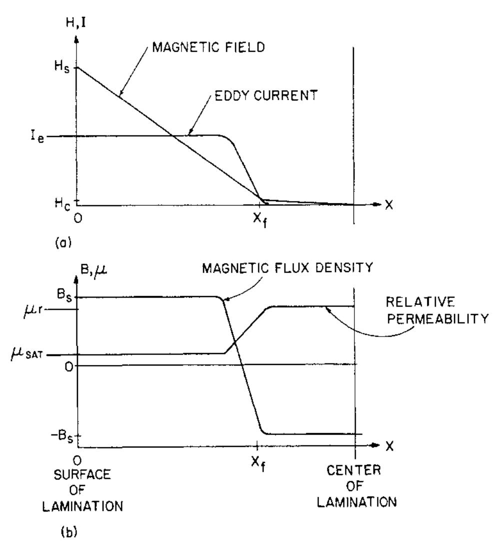

Fig. 7. Saturation parameter spatial distributions.

The switching time T_{sw} of a steel tape-wound magnetic core is the difference in the saturation times for the shortest and the longest magnetic paths in the core and is given by[1]

$$T_{sw} = t_L \left(\frac{B_s}{N_T \rho}\right)^{1/2} \left(\ell_o^{1/2} - \ell_i^{1/2}\right) \frac{\left[\int_0^t I(T)\,dT\right]^{1/2}}{I(t)} \quad , \qquad (4)$$

where B_s is the saturation flux density, ρ is the material resistivity, t_L is the lamination thickness, $I(t)$ is the current in the number of turns N_T of conductor surrounding the magnetic material, and ℓ_o and ℓ_i are the lengths of the outside (longest) and the inside (shortest) magnetic paths in the tape-wound core. The material parameters that affect the switching time are the lamination thickness and the material resistivity because B_s is chosen as large as possible to reduce the inductance and material volume. Thus, the switching time scales as $(t_L^2/\rho)^{1/2}$. The switching-time equation also indicates that the geometry is important in determining the switching performance. The number of stacked laminations or lamination windings should be designed to optimize the geometry factor by making the inside and outside magnetic path lengths similar, and the length of each should be minimized. Thus, a toroidal tape-wound magnetic core with a small inside radius and a large outside radius would have a much longer switching time than a toroidal core with inside and outside radius approximately equal.

Note that the magnetic cores in the low-inductance geometries of Fig. 6 are also designed for fast switching. The core-lamination stack height is limited so that the minimum and maximum magnetic path lengths are approximately equal. If more magnetic material is required, several identical cores are added.

Material Losses

The first-order analytical study indicates that the leakage current through the SFME is given by[1]

$$I_L(t) = \frac{1}{8} \left(\frac{t_L}{A_m}\right)^2 \left(\frac{\ell_a}{B_s N_T \rho}\right) V_a(t) \int_0^t V_a(t)\,dT \quad . \qquad (5)$$

Note that for a given magnetic material cross-sectional area A_m and an average magnetic path length $_a$, the leakage current scales as the lamination thickness t_L squared and inversely as the material resistivity . The eddy current energy loss E_e also scales as

$$E_e = \frac{1}{8} \left(\frac{t_L}{A_m}\right)^2 \left(\frac{\ell_a}{\rho N_T B_s}\right) \int_0^t V_a^2(s) \int_0^s V_a(r)\,dr\,ds \quad , \qquad (6)$$

such that the lamination thickness and the material resistivity are again the important parameters. The eddy current loss and the presaturation leakage current, both of which must be reduced to an acceptable value, scale as (t_L^2/ρ).

Spin relaxation damping losses are approximately equal to the eddy-current losses[2] and are not discussed in this paper. Anisotrophy or core losses are also neglected for the purpose of this paper.

Interlaminar Insulation

The driving magnetic field induces a back voltage around each lamination of magnetic material due to the changing magnetic flux. Thus, the potential difference between adjacent laminations must be insulated to prevent high conductivity eddy-current losses. The insulation thickness must be much less than the lamination thickness so that the majority of the composite cross section is magnetic material, or the stacking factor SF is close to unity. If all the lamination magnetic path lengths are approximately equal, the dielectric strength E_d of the lamination must be greater than

$$E_d \geq \frac{8B_sW_L}{T} \left(\frac{SF}{1-SF}\right) , \qquad (7)$$

where W_L is the lamination width, T is the resonant transfer period, and B_s is the material saturation flux density. Thus, the lamination width is chosen so the voltage between adjacent laminations is compatible with the dielectric strength of the interlaminar insulation. The material to be used for interlaminar insulation must withstand the annealing cycle for the magnetic material.

Material Selection

To reduce the presaturation leakage currents and the eddy-current losses, a thin lamination of high resistivity magnetic material is desired. Amorphous steel material can be fabricated with a minimum thickness of approximately 1 mil (0.001 in.). Therefore, in the 50-100-ns regime, nickel steel materials with thicknesses on the order of 0.1 mil must be used to reduce the eddy-current losses and leakage currents to acceptable levels. Because of similar scaling, a low-loss magnetic design will also switch fast. Amorphous steel materials with thicknesses on the order of 0.2 mil, if possible to fabricate, would be equivalent to the 0.1-mil NiFe materials.

The insulation material between adjacent laminations must have a thickness on the order of 0.01 mil for a stacking factor of 0.9. For peak system voltages in the 100-kV range compression periods of 50 ns and lamination width of 1 cm, the insulation must withstand a voltage on the order of 2.5 V or have a dielectric strength of 250 V/mil. This is possible with conventional insulation techniques for NiFe materials that can withstand the required annealing temperatures. Thus available, but expensive, NiFe materials may be used in short-pulse, high-voltage magnetic modulators for lasers and accelerators.

Saturable Stripline Transformer Design

The development of a low-inductance, voltage step-up transformer with a near-unity coupling prior to saturation and a fast saturation or switching time is essential if the parallel magnetic pulse compressor is to be used in high-voltage, short-pulse systems. The low-inductance conductor geometry and the fast switching magnetic geometries and materials discussed previously are directly applicable to a transformer design. Thus, the problem of obtaining a near-unity coupling coefficient prior to saturation is discussed. The effective permeability μ_e of the magnetic core can be determined by

$$\mu_e\mu_o = \frac{2\ SF}{t_L} \left(\frac{B_s\rho\, \ell_a}{N}\right)^{1/2} \left[\frac{\int_0^t i(T)\,dT}{i(t)}\right]^{1/2} . \qquad (8)$$

Note that the free scaling factor is $(t_L/\rho)^{-1/2}$, which should be maximized. The relative value for μ_e using 0.1-mil steel is on the order of 1000 at the voltages and times of interest. Thus, using the 0.1-mil 50-50 NiFe material can possibly provide sufficient coupling to minimize the energy loss to the transformer magnetizing inductance. An additional measure to increase the coupling prior to saturation is the use of skin currents to force flux channeling from primary to secondary.[1] A low-inductance, fast magnetic switching, saturable stripline transformer is shown in Fig. 8.

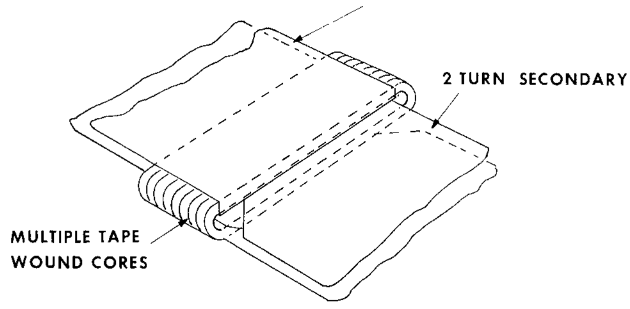

(a) BASIC 1:2 SATURABLE STRIPLINE TRANSFORMER

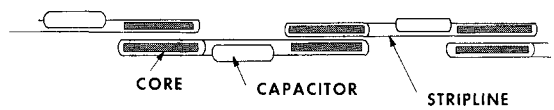

(b) SUCCESSIVE STAGE ARRANGEMENT

Fig. 8. Stripline magnetic modulator.

Conclusions

Several conclusions can be drawn from the initial magnetic modulator investigation.

1. Magnetic modulator systems can be designed to operate in the high-voltage (50-500 kV), short-pulse (50-100 ns) mode required by lasers and accelerators.
2. Low-inductance geometries are required to transfer and compress a specific energy at high voltages in short times.
3. The stripline geometry is essential to obtaining the low inductance required.
4. Magnetic switching times of several nanoseconds are possible.
5. Magnetic materials with thicknesses on the order of 0.1 to 0.2 mil are necessary to reduce leakage currents and eddy current losses to acceptable values. Thus, amorphous steel materials cannot be used for very short pulse magnetic switches.
6. Ferrite materials can be used for very short pulse magnetic compressors, but require approximately 10 times the volume of steel materials.

References

1. W. C. Nunnally, "Magnetic Switches and Circuits," Los Alamos National Laboratory report LA-8862-MS, (May 1981).
2. John E. L. Bishop, "The Shape, Energy, Eddy Current Loss and Relaxation Damping of Magnetic Domain Walls in Glassy Iron Wire," IEEE Trans. Magn. MAG-13, No. 5, 1638-1645 (September 1977).